Allosteric Modulation of the Cannabinoid CB$_1$ Receptor

Martin R. Price, Gemma L. Baillie, Adèle Thomas, Lesley A. Stevenson, Morag Easson, Richard Goodwin, Adèle McLean, Lorraine McIntosh, Gillian Goodwin, Glenn Walker, Paul Westwood, Julia Marrs, Fiona Thomson, Phillip Cowley, Arthur Christopoulos, Roger G. Pertwee & Ruth A. Ross.

School of Medical Sciences, Institute of Medical Sciences, University of Aberdeen, Aberdeen, AB25 2ZD. SCOTLAND. UK .(MRP, GLB, AT, LAS, RGP, RAR).

Organon Research, Newhouse, Lanarkshire, SCOTLAND. UK. (ME, RG, AM, LM, GG, GW, PW, JM, FT, PC).

Dept. of Pharmacology, University of Melbourne, Parkville, AUSTRALIA. (AC)

1

Running title: Allosteric modulation of the cannabinoid CB_1 receptor.

Correspondence and proofs to:

Dr R.A. Ross, School of Medical Sciences, Institute of Medical Sciences, University

of Aberdeen, Foresterhill, Aberdeen AB25 2ZD, SCOTLAND.UK

Telephone: +44 (0)1224-555705

Email: r.ross@abdn.ac.uk

Number of Pages: **33**

Number of Figures: **8**

Number of Tables: **5**

Number of References: **34**

Number of words: *Abstract* (**250**), *Introduction* (**710**), *Discussion* (**1552**)

(NB reviewers required additions to discussion)

Abbreviations:

Bovine serum albumin, BSA; Cannabinoid, CB; Dimethyl sulphoxide, DMSO; Guanine diphosphate, GDP; G protein-coupled receptor, GPCR; Guanine triphosphate, GTP; Ternary Complex Model, TCM.

Abstract

We investigated the pharmacology of three novel compounds, Org 27569, Org 27759 and Org 29647, at the cannabinoid CB_1 receptor. In equilibrium binding assays the Org compounds significantly increased the binding of the CB_1 receptor agonist [^{3}H]CP55940, indicative of a positively cooperative allosteric effect. The same compounds caused a significant, but incomplete, decrease in the specific binding of the CB_1 receptor inverse agonist, [^{3}H]SR141716A, indicative of a limited negative binding cooperativity. Analysis of the data according to an allosteric ternary complex model revealed that the estimated affinity of each Org compound was not significantly different when the radioligand was [^{3}H]CP55940 or [^{3}H]SR141716A. However, the estimated co-operatively factor for the interaction between modulator and radioligand was greater than 1 when determined against [^{3}H]CP55940 and less than 1 when determined against [^{3}H]SR141716A. [^{3}H]CP55940 dissociation kinetic studies also validated the allosteric nature of the Org compounds, since they all significantly decreased radioligand dissociation. These data suggest that the Org compounds bind allosterically to the CB_1 receptor and elicit a conformational change that increases agonist affinity for the orthosteric binding site. In contrast to the binding assays, however, the Org compounds behaved as insurmountable antagonists of receptor function; in the reporter gene assay, the [^{35}S]GTP S binding assay and the mouse vas deferens assay they elicited a significant reduction in the E_{max} value for CB_1 receptor agonists. The data presented clearly demonstrate, for the first time, that the cannabinoid CB_1 receptor contains an allosteric binding site that can be recognized by synthetic small molecule ligands.

Introduction

Mammalian tissues express at least two types of cannabinoid receptor, CB_1 and CB_2, both G protein coupled (reviewed in Howlett et al., 2002). CB_1 receptors are found predominantly at central and peripheral nerve terminals where they mediate inhibition of transmitter release. Endogenous ligands for these receptors also exist. These "endocannabinoids" are all eicosanoids, prominent examples including arachidonoylethanolamide (anandamide) and 2-arachidonoyl glycerol (2-AG), both of which are synthesised on demand, removed from their sites of action by tissue uptake processes and metabolised by intracellular enzymes (see Pertwee and Ross, 2002). There is ample evidence for a role of the endocannabinoid system in a number of physiological processes including cardiovascular regulation, appetite control, learning and memory and pain processing (reviewed in Di Marzo et al., 2004). Within the brain, the distribution of CB_1 receptors is heterogeneous, accounting for several well-documented pharmacological properties of CB_1 receptor agonists. For example, the cerebral cortex, hippocampus, lateral caudate-putamen, substantia nigra, pars reticulata, globus pallidus, entopeduncular nucleus and the molecular layer of the cerebellum are all populated with particularly high concentrations of CB_1 receptors. CB_1 receptor ligands have therapeutic potential in a range of disorders including obesity, nicotine addiction, pain, inflammation, gastrointestinal disorders, multiple sclerosis, psychosis, schizophrenia and osteoporosis.

The classical view of G protein-coupled receptor (GPCR) signalling posits that agonists initiate signalling by binding to a site on the GPCR that has specifically evolved to recognise the endogenous agonist for that receptor; this site has been

defined as the *orthosteric* binding site (Neubig et al., 2003). It is now recognised, however, that GPCRs may also contain *allosteric* binding sites for endogenous and/or synthetic ligands (Christopoulos and Kenakin, 2002). Allosteric sites are topographically distinct from the orthosteric site, hence the structural features that determine ligand binding to allosteric sites are different from those of orthosteric ligands. In contrast to the direct effects on receptor function that are mediated by orthosteric ligands, allosteric drugs act by modulating receptor activity through conformational changes in the receptor that are transmitted from the allosteric to the orthosteric site and/or to effector coupling sites (Christopoulos, 2002).

The simplest allosteric interaction can be described by the allosteric ternary complex model (TCM; Figure 1), where the effect of an allosteric ligand is to change the affinity of an orthosteric ligand for the receptor, and vice versa (Ehlert, 1988; Lazareno and Birdsall, 1995). Mechanistically, allosteric modulation of affinity reflects a conformational change in the receptor that may lead to an alteration in the dissociation kinetics of a preformed orthosteric ligand-receptor complex; this effect on dissociation kinetics cannot occur if interacting ligands recognize the same binding site, and is thus diagnostic of an allosteric effect (Kostenis and Mohr, 1996; Christopoulos, 2000). More recently, data have been presented to suggest that allosteric modulators may affect the *efficacy* of orthosteric ligands in addition to, or independently of, effects on orthosteric ligand binding, necessitating the development of more complex models of allosteric modulation (see Christopoulos and Kenakin, 2002, and references therein).

To date, the main principle underlying GPCR-based drug discovery has invariably been the optimisation of lead molecules towards the orthosteric site on the GPCR to obtain selectivity of action. However, allosteric modulators offer advantages

not readily available with orthosteric ligands. For example, allosteric drugs that affect affinity (but not efficacy) would be advantageous in that they would boost or dampen the effect of the endogenous ligand without disrupting the inherent spatial and temporal patterns of physiological signalling (May and Christopoulos, 2003). CB_1 receptor pharmacology is the subject of intense academic and commercial research effort directed at the treatment of obesity (Horvath, 2003), pain (Iversen and Chapman, 2002; Pertwee 2001), inflammation (Rice et al, 2001), osteoporosis (Idris et al, 2005), cancer (Bifulco & DiMarzo, 2002), multiple sclerosis (Pertwee, 2002) and cardiovascular disorders (Randall et al, 2002). There is ample evidence that the levels of endocannabinoids are altered in these pathophysiological situations. Allosteric enhancers of the cannabinoid CB_1 receptor would thus offer the prospect of producing clinically useful compounds that do not display the CNS side-effects that are characteristic of direct receptor agonism. In this investigation we provide the first evidence for an allosteric binding site on the cannabinoid CB_1 receptor, as revealed by the pharmacology and mode of action of a novel class of synthetic small molecules (Figure 2).

Material and Methods

Materials

(+) WIN55212 and CP55940 were obtained from Tocris and SR141716A [N-(piperidin-1-yl)-5-(4-chlorophenyl)-1-(2,4-dichlorophenyl)-4-methyl-1H-pyrazole-3-carboxamide hydrochloride] from the National Institute on Drug Abuse. Bovine serum albumin (BSA), Cell culture media, DTT, non-enzymatic cell dissociation solution, GDP, Gpp(NH)p, GTP S, G418, l-glutamine, Krebs salts, penicillin/streptomycin, Tris Buffer and Triton X-100 were all obtained from Sigma-

Aldrich. [^{3}H] CP55940 (128 Ci mmol^{-1}) and [^{35}S]GTP S (1250 Ci mmol^{-1}) were obtained from Amersham Pharmacia Biotech (UK). [^{3}H] SR141716A (44 Ci mmol^{-1}) was obtained from the National Institute on Drug Abuse. Three novel compounds from Organon research (*ORG 27569-0*: 5-Chloro-3-ethyl-1H-indole-2-carboxylic acid [2-(4-piperidin-1-yl-phenyl)-ethyl]-amide; *ORG 27759-0*: 3-Ethyl-5-fluoro-1H-indole-2-carboxylic acid [2-94-dimethylamino-phenyl)-ethyl]-amide; *ORG 29647-1*: 5-Chloro-3-ethyl-1H-indole-2-carboxylic acid (1-benzyl-pyrrolidin-3-yl)-amide, 2-enedioic acid salt).

Radioligand Binding Assays

Mouse Brain Membrane Preparation

Whole brains from adult male MF1 mice were suspended in centrifugation buffer (320 mM sucrose, 2 mM EDTA, 5 mM MgCl$_2$) and the tissues were homogenized with an Ultra-Turrex homogenizer. Tissue homogenates were centrifuged at 1600 g for 10 minutes and the resulting supernatant collected. This pellet was resuspended in centrifugation buffer centrifuged as before and the supernatant collected. Supernatants were combined before undergoing further centrifugation at 28,000 g for 20 minutes. The supernatant was discarded and the pellet resuspended in buffer A (50 mM Tris, 2 mM EDTA, 5 mM MgCl$_2$ at pH 7.0) and incubated at 37°C for 10 minutes. Following the incubation, the suspension was centrifuged for 20 minutes at 23,000 g. After resuspending the pellet in buffer A, the suspension was incubated for 40 minutes at room temperature before a final centrifugation for 15 minutes at 11,000 g. The final pellet was resuspended in buffer B (50 mM Tris, 1 mM EDTA, 3 mM MgCl$_2$) and the final protein concentration, determined by Bio-Rad Dc kit, was 1 mg ml^{-1}. All centrifugation procedures were

carried out at 4°C. Prepared brain membranes were stored at -80°C and defrosted on the day of the experiment.

Equilibrium Binding Assays

Binding assays were performed with the CB_1 receptor agonist, [3H]CP55940 (0.7 nM) and the CB_1 receptor antagonist, [3H]SR141716A (1.2 nM), 1 mg ml^{-1} bovine serum albumin (BSA) and 50 mM Tris buffer containing 0.1mM EDTA and 0.5mM $MgCl_2$ (pH 7.4), total assay volume 500 µl. Binding was initiated by the addition of mouse brain membranes (30 µg). Assays were carried out at 37 °C for 60 minutes before termination by addition of ice-cold wash buffer (50 mM Tris buffer, 1 mg ml^{-1} BSA) and vacuum filtration using a 24-well sampling manifold (Brandel Cell Harvester) and Whatman GF/B glass-fibre filters that had been soaked in wash buffer at 4°C for 24 h. Each reaction tube was washed five times with a 4-ml aliquot of buffer. The filters were oven-dried for 60 min and then placed in 5 ml of scintillation fluid (Ultima Gold XR, Packard), and radioactivity quantitated by liquid scintillation spectrometry. Specific binding was defined as the difference between the binding that occurred in the presence and absence of 1 µM of the corresponding unlabelled ligand and was 70 - 80% of the total binding.

Dissociation Kinetics

Dissociation kinetic assays were performed with the CB_1 receptor agonist, [3H]CP55940 (0.7 nM), 1 mg ml^{-1} bovine serum albumin (BSA) and 50 mM Tris buffer containing 0.1mM EDTA and 0.5mM $MgCl_2$ (pH 7.4), total assay volume 500 µl. We utilised the 'isotopic dilution' method to measure the dissociation rate constant for [3H]CP55940 from brain membranes (see Christopoulos, 2000). [3H]CP55940

(0.7nM) was incubated with mouse brain membranes (30 µg) for 60 minutes at 25°C. Dissociation was initiated by the addition of 1µM unlabelled ligand in the presence and absence of test compounds. Dissociation times of 0.5 to 120 minutes at 25°C were used. To determine the non-specific binding, experiments were also performed in the presence of 1µM of the unlabelled ligand. Binding was terminated by addition of ice-cold wash buffer (50 mM Tris buffer, 1 mg ml^{-1} BSA) and vacuum filtration using a 24-well sampling manifold (Brandel Cell Harvester) and Whatman GF/B glass-fibre filters that had been soaked in wash buffer at 4 °C for 24 h. Each reaction tube was washed five times with a 4-ml aliquot of buffer. The filters were oven-dried for 60 min and then placed in 5 ml of scintillation fluid (Ultima Gold XR, Packard), and radioactivity quantitated by liquid scintillation spectrometry. Specific binding was defined as the difference between the binding that occurred in the presence and absence of 1 µM unlabelled ligand and was 70 - 85% of the total binding.

Mouse Isolated Vas Deferens Assay

Vasa deferentia were obtained from albino MF1 mice weighing 26 to 40 g. Each tissue was mounted in a 4 ml organ bath at an initial tension of 0.5g. The baths contained Mg^{2+}-free Krebs solution which was kept at 35°C and bubbled with 95% O_2 and 5% CO_2. The composition of the Krebs solution was (mM): NaCl 118.2, KCl 4.75, KH_2PO_4 1.19, $NaHCO_3$ 25.0, glucose 11.0 and $CaCl_2$.$6H_2O$ 2.54. Isometric contractions were evoked by stimulation with 0.5 s trains of three pulses of 110% maximal voltage (train frequency 0.1Hz; pulse duration 0.5 ms) through a platinum electrode attached to the upper end and a stainless steel electrode attached to the lower end of each bath. Stimuli were generated by a Grass S48 stimulator, then amplified (Med-Lab channel attenuator) and divided to yield separate outputs to eight

9

organ baths (Med-Lab StimuSplitter). Contractions were monitored by computer using a data recording and analysis system (MacLab) that was linked via preamplifiers (Macbridge) to UF1 transducers. After placement in an organ bath, each tissue was subjected to a stimulation-free period of 15 min and then stimulated for 10 min. Tissues were then subjected to alternate periods of stimulation (5 min) and rest (10 min) until consistent twitch amplitudes were obtained. This equilibration procedure was followed by a stimulation-free period of 10 min. Tissues were then stimulated for 10 min after which the stimulator was switched off and the Org compound or its vehicle added. Thirty minutes later, the first addition of the non-selective CB_1/CB_2 receptor agonist, R-(+)-WIN55212 (WIN55212) was made. Additions of WIN55212 were made cumulatively at 5 min intervals without washout, the tissues being stimulated for the final two minutes of exposure to each concentration of this agonist. Org compounds were dissolved in DMSO and WIN55212 in a solution consisting of 50% DMSO and 50% saline. By themselves, these vehicles did not inhibit the twitch response. Drug additions were made in a volume of 10 µl.

The measured response was WIN55212-induced inhibition of electrically-evoked contractions of the mouse isolated vas deferens and the vehicle we used for WIN55212 was DMSO/saline (1:1). The Org compounds (or their vehicle, DMSO) were added 30 min before WIN55212 which was then added cumulatively using a 15-minute dose cycle. Thus we constructed WIN55212 concentration-response curves in the presence of DMSO or the Org compounds.

The degree of inhibition of evoked contractions induced by WIN55212 was calculated in percentage terms by comparing the amplitude of the twitch response after each addition of WIN55212 with its amplitude immediately before the first

addition of this agonist.

[^{35}S]GTPγS Binding Assay

Mouse brain membranes (5μg protein) were preincubated for 30 minutes at 30°C with adenosine deaminase (0.5 U ml^{-1}). The membranes were then incubated with the agonist with vehicle or modulator for 60 minutes at 30 °C in assay buffer (50 mM Tris-HCl; 50 mM Tris-Base; 5 mM MgCl$_2$; 1 mM EDTA; 100 mM NaCl; 1 mM DTT; 0.1% BSA) in the presence of 0.1 nM [^{35}S]GTP S and 30 µM GDP, in a final volume of 500 µl. Binding was initiated by the addition of [^{35}S]GTP S. Nonspecific binding was measured in the presence of 30 µM GTP S. The reaction was terminated by rapid vacuum filtration (50 mM Tris-HCl; 50 mM Tris-Base; 0.1% BSA) using a 24-well sampling manifold (cell harvester; Brandel, Gaitherburg, MD) and GF/B filters (Whatman, Maidstone, UK) that had been soaked in buffer (50 mM Tris-HCl; 50 mM Tris-Base; 0.1% BSA) for at least 24 hours. Each reaction tube was washed six times with a 1.2 ml aliquot of ice-cold wash buffer. The filters were oven-dried for at least 60 minutes and then placed in 5 ml of scintillation fluid (Ultima Gold XR, Packard). Radioactivity was quantified by liquid scintillation spectrometry.

CB$_1$ Reporter Gene Assay

Test compounds are all prepared in glass vials and were dissolved in DMSO to give a concentration of 10mM. The solutions were then diluted in Nut.Mix F-12 media with 3% BSA to give a range of concentrations from 0.1mM to 0.1nM (x10 stocks) for addition to the assay (BSA final concentration is 0.3%). The DMSO concentration did not exceed 0.1% by volume. For all aqueous solutions ultrapure water (Milli-Q quality) was used.

11

CHO cells, expressing the human CB_1 receptor were transfected with a luciferase reporter gene under the control of seven AP1 repeats (Stratagene). Single cell-derived clones were maintained in F12 Nut Mix (1:1) with 10% FetaClone II, penicillin/streptomycin 50U/50μg ml^{-1}, fungizone1μg ml^{-1}, geneticin (disulphate salt) 0.2μg ml^{-1}, hygromycin 0.5μg ml^{-1} at 37°C/5% CO_2. The day before the assay, the cells were harvested using trypsin-EDTA, then pelleted by centrifugation (5 minute, 20°C spin at 600g The pellet was resuspended in phenol red/serum free DMEM/F12 Nut Mix containing penicillin/streptomycin (50U/50μg ml^{-1}) and fungizone (1μg ml^{-1}). The cells were then seeded into white 96 well plates (Packard CulturPlates) at a density of $3x10^4$ cells per well (100 μl final volume). Cells were incubated overnight (approximately 18hrs at 37°C, 5%CO_2/95% air) prior to assay.

10μl of a x10 stock of test compound was added directly to the relevant wells and the plates incubated at 37°C for 5 hours and then under subdued light 100μl of LucLite reagent (reconstituted as per Packard's instructions) added to each well. The plates were covered with Top Seal and then incubated at room temperature for 5 minutes before counting on the Packard TopCount (single photon counting, 0.01 minute count time, no count delay). For modulator studies, the cells were pre-incubated for 5 minutes with the test compound and then agonist. Incubations and luciferase assays were then performed as detailed above.

Data Analysis

Radioligand competition binding isotherms for the interaction between orthosteric ligands were analyzed using Prism 4.01 (GraphPad Software, San Diego, CA) according to the following logistic function:

$$Y = \frac{(Top - Bottom)[I]}{[I] + IC_{50}} \qquad (1)$$

where Y denotes the percent specific binding, Top and Bottom denote the maximal and minimal asymptotes, respectively, [I] denotes the inhibitor concentration and IC_{50} denotes the inhibitor potency (midpoint location) parameter.

The interaction between each radioligand and the test modulators was analyzed according to the following allosteric ternary complex model of interaction:

$$Y = \frac{[A]}{[A] + \dfrac{K_A\left(1 + \dfrac{[B]}{K_B}\right)}{\left(1 + \dfrac{\alpha[B]}{K_B}\right)}} \qquad (2)$$

where Y denotes the fractional specific binding, [A] and [B] denote the concentration of orthosteric and allosteric ligands, respectively, K_A and K_B denote their respective equilibrium dissociation constants, and   denotes a cooperativity factor that governs the magnitude and direction of the allosteric interaction between the two ligands when they both occupy the receptor. For this analysis, values of [A] and K_A were fixed as constants (the latter determined from previous saturation binding assays), whereas values of   and K_B were determined by nonlinear regression.

For the dissociation kinetic experiments, the decay in radioligand binding over time was analyzed according to the following two-phase exponential decay model:

$$Y = Span1 \; e^{-k_1 \, t} + Span2 \; e^{-k_2 \, t} + Plateau \qquad (3)$$

where Span1 and Span2 denote the percentage of each phase, Plateau denotes the minimal asymptotic value, and k_1 and k_2 denote the rate constants for the components defined by Span1 and Span2, respectively. An extra-sum-of-squares (F-test) was used to determine whether the data were significantly better fitted to this model as compared to a simpler model characterized by a single Span and k value.

Concentration-response data were fitted empirically to the following four-parameter logistic equation:

$$Y = Basal + \frac{\left(E_{max} - Basal\right)[A]^{n_H}}{[A]^{n_H} \; + \; 10^{-pEC_{50} \; n_H}} \qquad (4)$$

where Y denotes effect, [A] the concentration of agonist, n_H the Hill slope, pEC_{50} the negative logarithm of the midpoint location parameter, and E_{max} and Basal the upper and lower asymptotes, respectively. An extra-sum-of-squares (F-test) was used to determine whether the data were significantly better fitted assuming separate values for the Basal and n_H parameters across each dataset in the absence relative to presence of test compound, compared to common values for each parameter.

In practice, all affinity (K_B), potency (EC_{50}) and cooperativity ( ) parameters were estimated as logarithms (Christopoulos, 1998).

Operational Model-Fitting

The functional interaction between test compounds and the orthosteric agonist, WIN 55,212-2, in the mouse isolated vas deferens was fitted to the following operational model of allosterism (see Appendix for derivation):

$$E = \frac{E_m \tau^n [A]^n \left(1 + \dfrac{\alpha\beta[B]}{K_B}\right)^n}{[A]\left(1 + \dfrac{\alpha[B]}{K_B}\right) + K_A\left(1 + \dfrac{[B]}{K_B}\right)^n + \tau^n[A]^n\left(1 + \dfrac{\alpha\beta[B]}{K_B}\right)^n} \tag{5}$$

where E denotes the effect,   denotes an empirical proportionality constant that quantifies the change in stimulus imparted to the receptor by the agonist in the presence of modulator, E_m denotes the maximum possible effect,   is an operational measure of orthosteric ligand efficacy, and n is a logistic slope factor that governs the shape of the stimulus-response function. [A], K_A and   are as defined above.

Statistics

Values have been expressed as means and variability as s.e.mean or as 95% confidence limits. Mean values have been compared using Student's unpaired t test or analysis of variance followed by Dunnett's test or the Newman-Keuls test. A P value <0.05 was considered to be significant.

Results

Equilibrium Binding Assays

In equilibrium binding experiments with the orthosteric agonist probe, [^{3}H]CP55940, unlabelled CP55940 competed with the radioligand according to a simple one-site competition model, characterized by a pIC_{50} value of 9.54 ± 0.09 (n = 5). In contrast, the test compounds all produced a significant, but saturable, *increase* in the level of specific [^{3}H]CP55940 binding (Figure 3A), the most marked effect being observed with Org 27569.

When the inverse agonist, [^{3}H]SR141716A, was used as the orthosteric probe, a different profile of activity was observed. As expected, unlabelled SR141716A displayed simple mass-action behaviour, competing with the radioligand and yielding a pIC_{50} value of 9.22 ± 0.02 (n = 4). Unlike their effects on agonist binding, the test compounds (at concentrations up to their solubility limit) also produced a significant decrease in the equilibrium binding of [^{3}H]SR141716A (Figure 3B). However, the reduction in specific radioligand binding mediated by the test compounds appeared saturable and incomplete, which is at odds with the expectations of simple competitive behaviour.

Both agonist and antagonist radiolabel binding data were fitted to the allosteric TCM (Figure 1; Equation 2), and the resulting parameters are shown in Table 1 where it can be seen that there is no significant difference in the estimated pK_B value for each compound at the putative allosteric site on the CB_1 receptor when tested against [^{3}H]CP55940 compared to when [^{3}H]SR141716A was used as the orthosteric probe. In contrast, the [^{3}H]CP55940 data were characterized by values greater than 1, indicative of a positive allosteric modulation of the binding of radiolabeled agonist,

16

whilst those of the [^{3}H]SR141716A dataset were less than 1, indicating a negative allosteric modulation of the binding of the inverse agonist.

Dissociation Kinetic Assays

In order to validate that the test compounds were, indeed, allosteric modulators of the CB$_1$ receptor, [^{3}H]CP55940 dissociation kinetic experiments were performed. In the absence of test compound, the dissociation of [^{3}H]CP55940 was significantly ($P<0.0001$; F-test) biphasic (Figure 4). The dissociation rate constants and the percentages for the two phases are listed in Table 2. When this experiment was performed in the presence of each of the test compounds, a concentration-dependent reduction was observed in each of the slow and fast radioligand dissociation rate constants (Figure 4A-C; Table 2), with no significant effect on the percentage of either phase. This finding is consistent with an alteration of receptor conformation that reduces orthosteric ligand dissociation without affecting G protein coupling status. In contrast, the addition of the non-hydrolysable GTP analogue, Gpp(NH)p (40µM), which is known to uncouple complexes between receptors and G-protein, did not have a significant effect on [^{3}H]CP55940 dissociation rates, but did significantly reduce the percentage of the slowly dissociating component of binding, from $59.03 \pm 3.03\%$ to $16.10 \pm 2.93\%$

Mouse Vas Deferens

The effects of the modulators on CB$_1$ receptor function were initially investigated using the mouse vas deferens as an in vitro model of CB$_1$ receptor activity. As shown in Figure 5A-C, the compounds by themselves neither inhibited

nor enhanced electrically-evoked contractions at the concentrations that were used (up to 1 µM), suggesting that they are neither allosteric agonists nor inverse agonists. This is in contrast to the effect of the established CB_1 receptor inverse agonist SR141716A, which significantly increases electrically-evoked contractions under the same assay conditions (Figure 5D). The functional effects of the compounds on the inverse agonism displayed by SR141716A in the mouse vas deferens is the subject of ongoing investigation.

When tested against the CB_1 agonist, WIN55212, an interesting effect was observed in the presence of modulator. Specifically, the maximal agonist effect (E_{max}) of WIN55212 to inhibit the electrically-evoked contractions of the mouse vas deferens was significantly reduced by each of Org 27569, Org 27759 and Org 29647, indicative of an insurmountable mode of antagonism (Table 3); with the exception of 1µM Org27569 and Org 27759, the compounds did not significantly alter the pEC_{50} values for WIN55212 (Table 3).

To investigate whether the effects of the compounds were unique to cannabinoid receptors, we conducted experiments with the $_2$ adrenoceptor agonist, clonidine. In the presence of DMSO, clonidine inhibited electrically-evoked contractions of the mouse vas deferens with a pEC_{50} of 9.00 ± 0.14 and E_{max} of 83 % (95% confidence limits 77.9 – 88.1). These values were not significantly different in the presence of 1µM of Org 27569, the pEC_{50} and E_{max} being 8.66 ± 0.11 and 77 % (95% confidence limits 70.6 – 82.7) respectively.

In order to gain further insight into the apparent dichotomy between modulators effects on agonist affinity, on the one hand, and efficacy, on the other, the data were globally fitted to an operational model of allosterism (see Appendix). This analysis was based on the following assumptions. First, WIN 55,212 was assumed to

be a full agonist at the CB_1 receptor (Pertwee, 1997): the E_{max} value of approximately 80% of the maximal tissue inhibition presumably represents the maximal inhibition that can be mediated by CB_1 receptor activation. Second, the G protein-coupled receptor active state, which is promoted by agonist binding, was assumed to be extremely transient, as expected for intact cells (Ehlert and Rathbun, 1990), such that the affinity estimate for WIN55212 reflected its K_A value for the uncoupled form of the receptor.

The results of this analysis are shown in Figure 6 and Table 4, and allow us to reconcile our observations with a mechanism whereby the binding cooperativity (value) between each modulator and WIN55,212 is positive, consistent with the enhancement of agonist binding observed in the [³H]CP55940 binding experiments, but the signalling efficiency of the ARB ternary complex (Figure 1) is significantly impaired (values tend towards or equal 0). Together, these two mechanisms can account for an insurmountable antagonism of receptor function with minimal effect on full agonist potency.

[³⁵S]GTPγS Binding Assay

The insurmountable antagonism mediated by the modulators in the intact mouse vas deferens functional assay is also evident when receptor activity is monitored using a more proximal measure of receptor-effector coupling. In the presence of vehicle, CP55940 produced a stimulation of [³⁵S]GTP S binding that was 78.65 % (95% confidence limits 66.7 – 90.6) above basal binding with a pEC_{50} value of 7.93 ± 0.14 (Figure 7A). In the presence of 100nM Org 29647, the curve was shifted to the right, although there was no statistically significant effect on E_{max} or pEC_{50}, these values being 73.70% (95% confidence limits 36.8 – 110) and 7.54 ±

0.48, respectively. However, when the concentration of Org 29647 was increased to 1µM, the ability of CP55950 to stimulate [^{35}S]GTP S turnover was completely abrogated.

In the presence of vehicle the endogenous cannabinoid, anandamide, produced a stimulation of [^{35}S]GTP S binding that was 61.1 % (95% confidence limits 53.8 – 68.3) above basal binding with a pEC$_{50}$ value of 6.62 ± 0.15 (Figure 7B). In the presence of 100nM Org 27569, the curve was shifted to the right, although there was no statistically significant effect on E$_{max}$ of 59.8 % (95% confidence limits 49.9 – 69.6). However, when the concentration of Org 27569 was increased to 1µM, the ability of anandamide to stimulate [^{35}S]GTP S turnover was significantly attenuated, the E$_{max}$ being 17.0 % (95% confidence limits 10.2 – 23.7).

Human CB$_1$ Receptor Reporter Gene Assay

To confirm that the effect of the modulators was not species-specific, additional functional assays were performed using cloned human CB$_1$ receptors. In the luciferase reporter assay, the Org compounds all behaved as insurmountable antagonists of CP55940 (Figure 8), causing a concentration-dependent reduction in the agonist E$_{max}$ value (see Table 5).

Discussion

The Org compounds that we have identified display a number of characteristics commonly associated with allosteric modulators, including i) either enhancement or inhibition of orthosteric CB_1 ligand binding depending on the nature of the orthosteric probe, ii) a slowing of the dissociation rate constant(s) for [^{3}H]CP55940 from the occupied CB_1 receptor and iii) a non-competitive inhibition of CB_1 receptor orthosteric agonist efficacy.

In equilibrium binding assays the Org compounds significantly increased the binding of the CB_1 receptor agonist [^{3}H]CP55940, indicative of a positively cooperative allosteric effect. In contrast, the same compounds caused a significant, but incomplete, decrease in the specific binding of the CB_1 receptor inverse agonist, [^{3}H]SR141716A, indicative of a limited negative binding cooperativity (Christopoulos and Kenakin, 2002). The most common mechanistic description of inverse agonism is based on the premise that GPCRs exist in at least 2 conformational states, an inactive R and an active R* state (Pertwee 2005). In this model, agonists have higher affinity for the R* state and shift the equilibrium towards R* resulting in G protein activation and an increase in GDP/GTP exchange. In contrast, inverse agonists bind preferentially to the R state, resulting in a decrease in constitutive activity. We used [^{3}H]CP55940 to selectively label the R* state, most likely present as the complexed R*G state in our membrane-based assays, and [^{3}H]SR141716A to label the R state of the receptor. Analysis of the data according to the allosteric TCM revealed that the estimated pK_B values for the Org compounds were not significantly different when the radioligand was [^{3}H]CP55940, or [^{3}H]SR141716A (Table 1). Because these affinity values represent the dissociation constant for the modulator binding to the allosteric site on the free (non orthosteric ligand-bound) receptor, they should indeed be independent of the orthosteric radioligand that is used (Lazareno and Birdsall, 1995). Additionally, since our orthosteric radioligands labelled specific receptor states, our analysis indicates that under the current

21

assay conditions, the binding of the allosteric modulators is not influenced appreciably by the

G protein coupling status of the receptor. The differences in the effects of each modulator on

the binding of the orthosteric ligands could thus be adequately described and quantified by the

estimated   values (Table 1) which were all greater than 1 when determined against the

binding of [^{3}H]CP55940 and less than 1 when determined against the binding of

[^{3}H]SR141716A. Cooperativity is known to be influenced by the nature of the ligand binding

to the orthosteric site, and it is thus not surprising that the   values are different for each

modulator, as well as between each modulator and either an agonist or antagonist probe (May

and Christopoulos, 2003).

Importantly, dissociation kinetic studies using [^{3}H]CP55940 as the probe also

validated the allosteric nature of the Org compounds, since they all significantly decreased the

dissociation rate constants for the radioligand. An alteration of the dissociation of a preformed

orthosteric ligand-receptor complex by a second ligand unambiguously demonstrates an

allosteric interaction (Kostenis and Mohr, 1996). Interestingly, [^{3}H]CP55940 displayed

biphasic dissociation kinetics, reflecting the presence of at least two receptor conformations

(Devlin and Christopoulos, 2002). The rapidly dissociating component of [^{3}H]CP55940

binding likely represents binding to the low affinity uncoupled receptors (R) while the slowly

dissociating component possibly reflects binding to high affinity activated (R*) receptors.

Irrespective of the actual nature of the receptor states detected in the dissociation assays, the

Org compounds significantly decreased the dissociation rate constant for both the slow and

fast components of agonist binding without significantly affecting the proportion of each state.

The compounds therefore modulate the dissociation of [^{3}H]CP55940 from both the R and R*

receptor conformations. A reduction in the dissociation rate constant is in line with the

positive cooperativity observed in the equilibrium binding assay of [^{3}H]CP55940. Taken

together, these data suggest that the Org compounds bind allosterically to the CB$_1$ receptor

and elicit a conformational change that increases agonist affinity for the orthosteric binding site.

Despite the positive allosteric enhancement of agonist binding observed in the radioligand binding assays, perhaps the most striking observation from our study was the dissimilitude between the effect on binding affinity and the effect of the same modulators on agonist function (i.e. efficacy). In contrast to the binding assays, the Org compounds did not behave as allosteric enhancers but, rather, as insurmountable antagonists of receptor function; in the reporter gene assay, the $[^{35}S]GTP S$ binding assay and the mouse vas deferens assay they elicited a significant reduction in the E_{max} value for CB_1 receptor agonists. The effects of the modulators on function were specifically manifested at the receptor when it was dually occupied by both orthosteric and allosteric ligand, since there was no evidence of agonist or inverse agonist properties of the modulators when tested alone (Figure 5).

There are a number of examples in the recent literature of allosteric modulators that have profound inhibitory effects on orthosteric ligand efficacy while having minimal effects on orthosteric ligand binding (Litschig et al., 1999; Zahnet al., 2002; Watson et al., 2005), but our study is the first to reveal a striking difference between the magnitude and direction of allosteric modulation of orthosteric affinity, on the one hand, and efficacy, on the other. Numerous models have been proposed to specifically account for such behaviour at the molecular level (e.g. Hall, 2000; Christopoulos and Kenakin, 2002; Parmentier et al., 2002). A key feature of these models is that they contain multiple receptor states that are differentially stabilized by both orthosteric and allosteric ligands. As a consequence, the type of probe and the nature of the assay used can bias the detection of one set of receptor states over another and hence lead to a situation such as that described in our study where different observations are made depending on the experimental endpoint.

These findings have highly significant implications for drug discovery based on allosteric modulators, since they highlight the possibility of misclassification of novel ligands if they are not tested in as full a spectrum of biological assays as possible. In this regard, the operational model of allosterism, as presented in our study, can prove particularly useful. Like the molecular models described in the preceding paragraph, the operational model we have used is able to accommodate effects of allosteric modulators on both binding and function. However, the operational model has the additional advantage of containing fewer parameters than the molecular models; to our knowledge, this is the first application of such a model to derive quantitative functional parameter estimates for allosteric modulators (Table 4). The operational model parameters K_A, K_B and   have the same mechanistic meaning as they would in any molecular model of allosterism, and their determination can lead to useful information for structure-activity studies. Although the parameter, , is used only as an empirical proportionality constant, its value can also provide useful insights. For example, values significantly different to either 1 or 0 would be indicative of a ternary complex (ARB) species that retains the ability to signal in the presence of modulator, but in a modified way.

One point of divergence between the functional and the binding data is with respect to the apparent affinity of the modulators for the mouse CB_1 receptor; in the vas deferens bioassay, the estimated affinity of the Org compounds was higher than that estimated in the binding assay (Table 1 versus Table 4). At the moment, the basis for this discrepancy between functional and binding affinity estimates remains unknown. However, a previous study by Pedder et al. (1991) revealed a striking divergence in the affinity estimates of the allosteric modulator, gallamine, at M_2 muscarinic receptors depending on the assay conditions used to determine this value. Indeed, differences in the affinity of the modulator spanned almost two orders of magnitude. It is also worth noting that these same variations in assay conditions had minimal effects on orthosteric ligand affinity estimates (Pedder et al.,

1991). Because allosteric sites are, by their very nature, topographically distinct from the orthosteric site on a GPCR, they can be sensitive to ionic changes under conditions where orthosteric ligands are minimally affected. Such a scenario could explain the discrepancy between the pK_B values obtained from our equilibrium binding (Table 1) and those obtained in the functional assay in the mouse vas deferens (Figure 6).

Taken together, our findings highlight the prospect of manipulating structure-activity to produce compounds that are either allosteric enhancers or allosteric antagonists of the CB_1 receptor. Endocannabinoid levels are significantly increased in models of both inflammatory and neuropathic pain and CB_1 receptor agonists are highly effective analgesics in these models (see Rice et al, 2001; Iversen and Chapman, 2002; Pertwee 2001). Furthermore, inhibitors of FAAH, the enzyme responsible for the rapid intracellular hydrolysis of anandamide, are antinociceptive in models of both inflammatory and neuropathic pain. These compounds do not display the CNS side-effects that are characteristic of direct CB_1 receptor agonism (Cravatt and Lichtman, 2004). Allosteric modulators of the cannabinoid CB_1 receptor would also offer the prospect of producing clinically useful compounds that do not display CNS side-effects.

In conclusion, this investigation has provided the first evidence for an allosteric binding site on the cannabinoid CB_1 receptor. This site can be recognized by synthetic small molecules and offers the prospect of a new avenue of CB_1 receptor research that will complement the existing portfolio of selective direct agonists and competitive antagonists.

REFERENCES

Bifulco M. & Di Marzo V (2002). Targeting the endocannabinoid system in cancer therapy: A call for further research *Nature Med.* **8**: 547 – 550.

Black JW and Leff P (1983) Operational models of pharmacological agonism. *Proc. Roy. Soc. (Lond.) B.* **220**:141-162.

Christopoulos A (1998) Assessing the distribution of parameters in models of ligand-receptor interaction: to log or not to log. *Trends in Pharmacol. Sci.***19**:351-357.

Christopoulos A (2000) Quantification of allosteric interactions at G protein-coupled Receptors using radioligand binding assays, in *Current Protocols In Pharmacology* (Enna SJ ed) pp 1.22.1-1.22.40, Wiley and Sons, NY.

Christopoulos A (2002) Allosteric binding sites on cell-surface receptors: novel targets for drug discovery. *Nat Rev Drug Discov* **1**:198-210.

Christopoulos A, Kenakin T. (2002). G protein-coupled receptor allosterism and complexing. *Pharmacol Rev* **54**: 323-374

Cravatt BF, Lichtman AH (2004). The endogenous cannabinoid system and its role in nociceptive behavior. *J Neurobiol* **61**: 149-160.

Devlin MG, Christopoulos A. (2002). Modulation of cannabinoid agonist binding by 5-HT in the rat cerebellum. *J Neurochem* **80**: 1095-1102

Di Marzo V, Bifulco M, De Petrocellis L. (2004). The endocannabinoid system and its therapeutic exploitation. *Nat Rev Drug Discov* **3**: 771-784.

Ehlert FJ (1988) Estimation of the affinities of allosteric ligands using radioligand binding and pharmacological null methods. *Mol. Pharmacol.* **33**:187-194.

Ehlert FJ and Rathbun BE (1990) Signaling through the muscarinic receptor-adenylate cyclase system of the heart is buffered against GTP over a range of concentrations. *Mol. Pharmacol.* **38**:148-158.

Furchgott RF (1966) The use of -haloalkylamines in the differentiation of receptors and in the determination of dissociation constants of receptor-agonist complexes. *Adv. Drug Res.* **3**:21-55.

Horvath T.L. (2003) Endocannabinoids and the regulation of body fat: the smoke is clearing *J Clin Invest.* **112**: 323–326.

Howlett AC, Barth F, Bonner TI, Cabral G, Casellas P, Devane WA, Felder CC, Herkenham M, Mackie K, Martin BR, Mechoulam R, Pertwee RG (2002). International Union of Pharmacology. XXVII. Classification of cannabinoid receptors. *Pharmacol Rev* **54**: 161-202.

Idris AI, van't Hof RJ, Greig IR, Ridge SA, Ross RA, Ralston SH. (2005). Regulation of bone mass, bone loss and osteoclast activity. *Nature Med.* **11**: 774 - 779.

Iversen L, Chapman V. (2002). Cannabinoids: a real prospect for pain relief*? Curr Opin Pharmacol* **2**: 50-55.

Kenakin T and Beek D (1982) *In vitro* studies on the cardiac activity of prenalterol with reference to use in congestive heart failure. *J. Pharmacol. Exp. Ther.* **220**:77-85.

Kostenis E and Mohr K (1996) Two-point kinetic experiments to quantify allosteric effects on radioligand dissociation. *Trends Pharmacol Sci* **17**:280-283.

Lazareno S and Birdsall NJM (1995) Detection, quantitation, and verification of allosteric interactions of agents with labeled and unlabeled ligands at G protein-coupled receptors: interactions of strychnine and acetylcholine at muscarinic receptors. *Mol. Pharmacol.* **48**:362-378.

Litschig S, Gasparini F, Rueegg D, Stoehr N, Flor PJ, Vranesic I, Prezeau L, Pin JP, Thomsen C and Kuhn R (1999) CPCCOEt, a noncompetitive metabotropic glutamate receptor 1 antagonist, inhibits receptor signaling without affecting glutamate binding. *Mol Pharmacol* **55**:453-461.

May LT, Christopoulos A. (2003). Allosteric modulators of G-protein-coupled receptors. *Curr Opin Pharmacol* **3**: 551-556.

Neubig RR, Spedding M, Kenakin T and Christopoulos A (2003) International Union of Pharmacology Committee on Receptor Nomenclature and Drug Classification. XXXVIII. Update on Terms and Symbols in Quantitative Pharmacology. *Pharmacol Rev* **55**:597-606.

Parmentier ML, Prezeau L, Bockaert J and Pin JP (2002) A model for the functioning of family 3 GPCRs. *Trends Pharmacol Sci* **23**:268-74.

Pedder EK, Eveleigh P, Poyner D, Hulme EC, Birdsall NJM (1991). Modulation of the structure-binding relationships of antagonists for muscarinic acetylcholine receptor subtypes. *Br. J.Pharmacol.* **103**:1561-1567.

Pertwee RG (2001). Cannabinoid receptors and pain. *Prog. Neurobiol.* **63**: 569 – 611.

Pertwee RG (2005). Inverse agonism and neutral antagonism at cannabinoid CB_I receptors. *Life Sci* **76**: 1307-1324

Pertwee RG, Ross RA. (2002). Cannabinoid receptors and their ligands. *Prostag Leukotr Ess Fatty Acids* **66**: 101-121

Pertwee RG (2002). Cannabinoids and multiple sclerosis. *Pharmacol Ther.* **95**:165-74.

Pertwee RG. (1997) Pharmacology of cannabinoid CB_1 and CB_2 receptors. *Pharmacol Ther.* 74:129-80.

Randall MD, Harris D, Kendall DA, Ralevic V.(2002). Cardiovascular effects of cannabinoids. *Pharmacol Ther*. **95**:191-202.

Rice, A.S.C., Farquhar-Smith, W.P. & Nagy, I. (2002). Endocannabinoids and pain: spinal and peripheral analgesia in inflammation and neuropathy. *Prostaglandins Leukotrienes and Essential Fatty Acids*, **66**:243-256.

Ross RA (2003). Anandamide and vanilloid TRPV1 receptors. *Brit J Pharmacol* **140**: 790.

Watson C, Jenkinson S, Kazmierski W and Kenakin T (2005) The CCR5 Receptor-Based Mechanism of Action of 873140, a Potent Allosteric Noncompetitive HIV Entry Inhibitor. *Mol Pharmacol* **67**:1268-82.

Zahn K, Eckstein N, Trankle C, Sadee W and Mohr K (2002) Allosteric modulation of muscarinic receptor signaling: alcuronium- induced conversion of pilocarpine from an agonist into an antagonist. *J Pharmacol Exp Ther* **301**:720-8

Figure Legends

Figure 1: The allosteric Ternary Complex Model (TCM), where R denotes the receptor, A and B denote the orthosteric and allosteric ligands, respectively, K_A and K_B denote their respective equilibrium dissociation constants, and   denotes a cooperativity factor that governs the magnitude and direction of the allosteric interaction between the two ligands when they both occupy the receptor. Values of greater than 1 denote positive binding cooperativity (enhanced affinity), values less than 1 denote negative binding cooperativity, and values equal to 1 denote neutral binding cooperativity.

Figure 2: The structure of Organon compounds. *ORG 27569-0*: 5-Chloro-3-ethyl-1H-indole-2-carboxylic acid [2-(4-piperidin-1-yl-phenyl)-ethyl]-amide; *ORG 27759-0*:   3-Ethyl-5-fluoro-1H-indole-2-carboxylic acid [2-94-dimethylamino-phenyl)-ethyl]-amide; *ORG 29647-1*:   5-Chloro-3-ethyl-1H-indole-2-carboxylic acid (1-benzyl-pyrrolidin-3-yl)-amide, 2-enedioic acid salt.

Figure 3: Equilibrium binding of (a) [^{3}H]CP55940 (0.7 nM) and (b) [^{3}H]SR141716A (1.2 nM) in mouse brain membranes in the presence of unlabelled ligand or the Org 27569, Org 29647 and Org 27759. Each symbol represents the mean percent specific binding $\pm$ the s.e.mean (n = 4 - 6). *P<0.05 and ***P<0.001, one-sample t-test. Curves superimposed on the data represent the best fits of Equation 1 (orthosteric ligands) or Equation 2 (allosteric modulators).

31

Figure 4: Dissociation of [^{3}H]CP55940 (0.7 nM) in mouse brain membranes in the presence of vehicle or (a) Org 27569 (b) Org 27759 (c) Org 29647 or (d) Gpp(NH)p. Each symbol represents the mean percent specific binding ± the s.e.mean (n = 4 - 8).

Figure 5: The effect of the Org compounds (a-c) and SR141716A (d) on the height of electrically-evoked contractions of the mouse isolated vas deferens. The figures show the g tension before adding either vehicle (DMSO) or drug ± s.e.mean. *P<0.05, **P<0.01, ***P<0.001, Student's unpaired t-test.

Figure 6: Inhibition of electrically-evoked contractions of the mouse isolated vas deferens by WIN55212 in the presence of the indicated Org compounds. Each symbol represents the mean percent inhibition ± the s.e.mean (n = 6- 8). Curves superimposed on the data represent the best global fit of the operational model of allosterism (Equation 5).

Figure 7: The stimulation of binding of [^{35}S]GTP S to mouse brain membranes by (A) CP55940 in the presence of vehicle (DMSO) or Org29647 and (B) anandamide in the presence of vehicle (DMSO) or Org27569. Each symbol represents the mean percent stimulation above basal ± the s.e.mean (n = 3 - 5).

Figure 8: Effect of Org compounds on enhancement of luciferase expression by CP55940 in CHO cells which stably express the human cannabinoid CB$_1$ receptor that have been co-transfected with a luciferase reporter gene which is under the regulatory control of a AP1-response element. Each symbol represents the mean percent of control stimulation (10µM CP55940) ± the s.e.mean (n = 3).

Footnotes

Table 1   Allosteric TCM binding parameters for various modulators at mouse brain CB_1 receptors.

Radioligand	Parameter	Allosteric Modulator		
		Org 27569	Org 27759	Org 29647
[3H] CP55940	pK_B [a]	5.67 ± 0.23	6.31 ± 0.32	5.78 ± 0.26
	Log [b]	1.14 ± 0.17	0.47 ± 0.10	0.44 ± 0.07
	[c]	$14\ (9.3 - 20.4)$	$3\ (2.3 - 3.7)$	$2.8\ (2.3 - 3.2)$
[3H] SR141617A				
	pK_B	5.95 ± 0.14	6.21 ± 0.14	5.84 ± 0.18
	Log	-1.04 ± 0.25	-0.48 ± 0.10	-0.44 ± 0.16
		$0.09\ (0.05 - 0.16)$	$0.33\ (0.26 - 0.42)$	$0.36\ (0.25 - 0.52)$

[a] Negative logarithm of the equilibrium dissociation constant for the allosteric modulator at the free receptor, determined using nonlinear regression according to Equations 2 of the Methods. Values represent the mean ± standard error of the mean of 4-8 experiments. For these analyses, the negative logarithm of the K_A value (Equation 2) was fixed to 9 for each radioligand, based on previous saturation binding assays.

[b] Logarithm of the cooperativity factor. All other details as for [a] above.

[c] Antilogarithm (geometric mean) of the cooperativity factor with range in brackets, based on the estimated Log values.

Table 2   Dissociation rate constants for [³H] CP55940 at mouse brain CB_1 receptors in the absence or presence of allosteric modulators [a].

	k_1 (slow) [b] ($\times 10^{-2}$ min⁻¹)	Half-life slow (min)	k_2 (fast) [c] (min⁻¹)	Half-life fast (min)
Vehicle	1.40 ± 0.08	49.4 (55.6 – 44.5)	0.294 ± 0.037	2.35 (3.14 – 1.88)
Org 27569 (100nM)	0.79 ± 0.03**	87.8 (94.2 – 82.2)	0.091 ± 0.006**	7.59 (8.69 – 6.74)
Org 27569 (1µM)	0.36 ± 0.03**	194 (235 – 165)	0.056 ± 0.005**	12.43 (15.31 – 10.44)
Org 27759 (1µM)	0.64 ± 0.03**	108 (119 – 99)	0.099 ± 0.008**	7.03 (8.29 – 6.11)
Org 27759 (10µM)	0.28 ± 0.03**	249 (304 – 210)	0.042 ± 0.004**	16.36 (19.6 – 14.03)
Org 29647 (1µM)	0.98 ± 0.04**	71.0 (76.5 – 66.2)	0.344 ± 0.026	2.01 (2.36 – 1.75)
Org 29647 (10µM)	0.26 ± 0.004**	264 (369 – 205)	0.036 ± 0.005**	19.53 (26.01 – 15.64)

[a] Parameter values were estimated using global nonlinear regression analysis, with the minimal plateau value constrained to 0. An extra-sum-of-squares (F-test) revealed that all datasets were adequately fitted assuming common values for the percentage of the slowly dissociating state (Span 1= 59.03 ± 3.03 %) and the fast dissociating state (Span 2 = 35.75 ± 2.97 %).

[b] Dissociation rate constant for the slowly dissociating state.

[c] Dissociation rate constant for the fast dissociating state.

**P<0.01, one-way ANOVA followed by Dunett's post test.

Table 3 Potency and maximal effect estimates for the inhibition of electrically-evoked contractions of the mouse vas deferens by WIN55212.

	pEC_{50} [a]	E_{max} [b] (%) (95% confidence limits)
DMSO	8.78 ± 0.083	82.7 (78.1 – 87.4)
Org 27569 (100 nM)	8.64 ± 0.11	58.4 (54.6 – 62.1)
Org 27569 (1 μM)	8.24 ± 0.12 **	45.4 (42.0 – 48.9)
DMSO	8.80 ± 0.095	83.9 (78.5 – 89.3)
Org 27759 (100 nM)	9.02 ± 0.122	65.2 (60.5 – 69.9)
Org 27759 (1 μM)	7.79 ± 0.171**	40.8 (35.7 – 45.9)
DMSO	8.94 ± 0.131	90.0 (59.9 – 73.2)
Org 29647 (100 nM)	8.79 ± 0.267	66.5 (59.9 – 73.2)
Org 29647 (1 μM)	8.82 ± 0.251	57.2 (52.1 – 62.2)

[a] Negative logarithm of the agonist EC_{50} value, determined using nonlinear regression analysis according to equation 4 of the Methods.

[b] Maximal agonist effect, determined using nonlinear regression analysis according to equation 4 of the Methods.

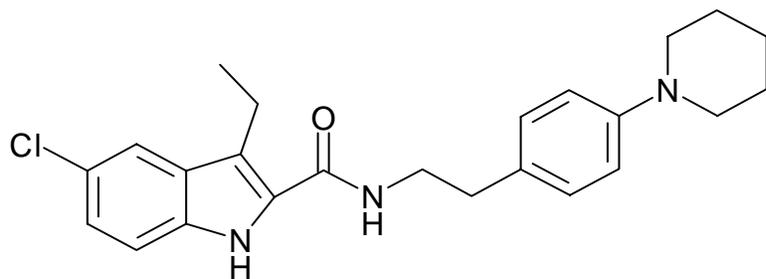**P < 0.01, on-way ANOVA followed by Dunnet's post test.

Table 4   Allosteric Operational Model binding parameters for various modulators at mouse vas deferens CB_1 receptors.

Parameter	Allosteric Modulator		
	Org 27569	**Org 27759**	**Org 29647**
pK_B [b]	7.57 ± 0.15	6.87 ± 0.28	7.46 ± 0.32
Log [c]	1.20 ± 0.15	1.32 ± 0.27	1.35 ± 0.19
[d]	$16 (11.2 - 22.4)$	$21 (11.2 - 38.9)$	$22 (14.4 - 34.7)$
[e]	0.006 ± 0.002	0 ± 0.002	0.018 ± 0.007

[a] All datasets (shown in Fig. 6) were globally analyzed using Equation 5 of the Methods. The best-fit parameter values describing the activity of WIN55212-2 across the datasets were as follows: $pK_A = 6.86 \pm 0.28$; Log $= 1.97 \pm 0.33$; $E_m = 82.7 \pm 3.6$; $n = 0.86 \pm 0.18$

[b] Negative logarithm of the equilibrium dissociation constant for the allosteric modulator at the free receptor, determined using nonlinear regression according to Equations 2 of the Methods. Values represent the mean ± standard error of the mean of 4-8 experiments.

[c] Logarithm of the cooperativity factor. All other details as for [a] above.

[d] Antilogarithm (geometric mean) of the cooperativity factor, based on the estimated Log   values.

[e] Empirical coupling constant, quantifying the fractional stimulus imparted by the modulator-occupied ternary complex.

Table 5 Potency and maximal effect estimates for the stimulation of luciferse reporter gene activity by CP55940 in hCB$_1$-expressing CHO cells

Modulator	Parameter	Modulator Concentration						
		0 (Vehicle)	3nM	10nM	30nM	100nM	300nM	1µM
Org 27569	E_{max} [a]	123 (118 – 127)	-	-	135 (132 – 138)	93 (91 – 96)	46 (45 – 48)	3.81 (3.45 – 4.17)
	pEC_{50} [b]	8.29 ± 0.07	-	-	8.67 ± 0.04**	9.01 ± 0.05**	9.30 ± 0.09**	-
Org 27759	E_{max}	103 (100 – 106)	104 (102 – 106)	93 (91 – 95)	69 (68 – 71)	26 (25 – 27)	-	-
	pEC_{50}	8.22 ± 0.06	8.45 ± 0.03*	8.56 ± 0.04**	8.80 ± 0.04**	9.50 ± 0.08**	-	-
Org 29647	E_{max}	105 (101 – 109)	105 (100 – 109)	108 (104 – 111)	90 (87 – 92)	52 (50 – 54)	25 (23 – 26)	4.75 (4.16 – 5.33)
	pEC_{50}	8.59 ± 0.07	8.67 ± 0.08	8.56 ± 0.06	8.73 ± 0.06	9.17 ± 0.08**	9.58 ± 0.12**	-

[a] Maximal agonist effect, determined using nonlinear regression analysis according to equation 4 of the Methods.

[b] Negative logarithm of the agonist EC_{50} value, determined using nonlinear regression analysis according to equation 4 of the Methods.
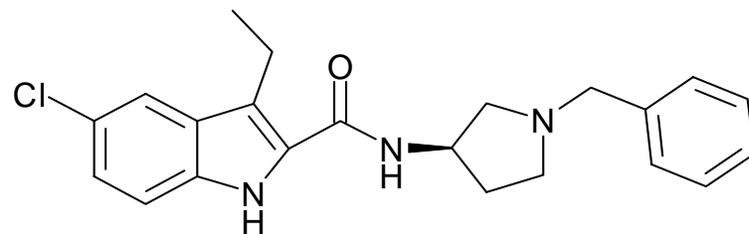
**P < 0.01, one-way ANOVA followed by Dunnet's post test.

Figure 1

$$K_B/\alpha$$

$$AR \rightleftharpoons ARB$$

$$K_A \qquad\qquad K_A/\alpha$$

$$R \rightleftharpoons RB$$

$$K_B$$
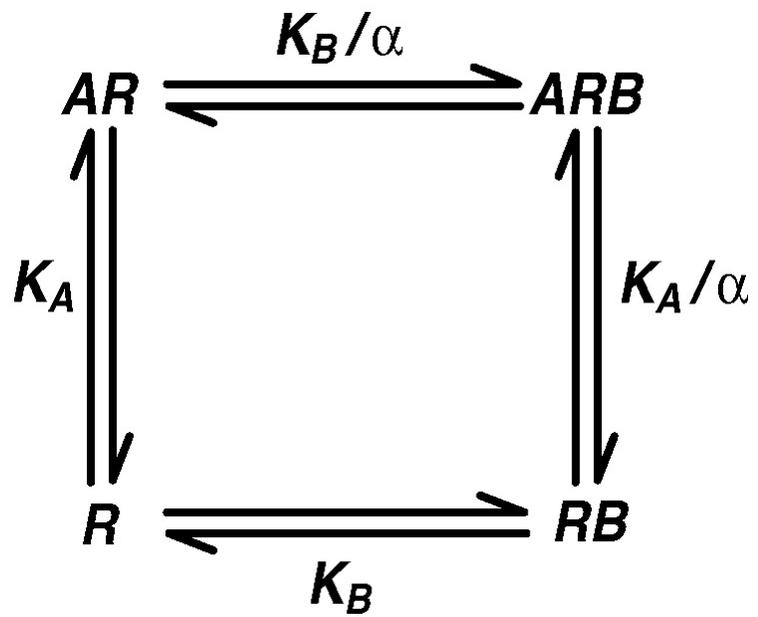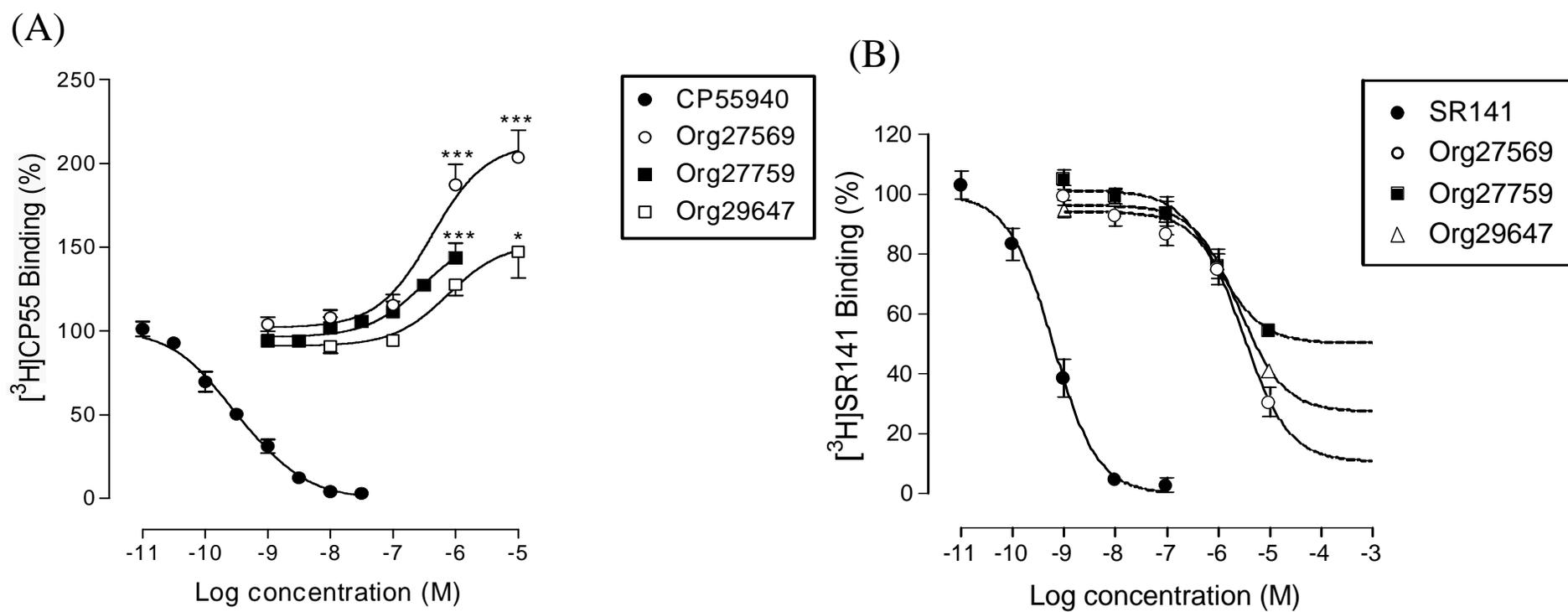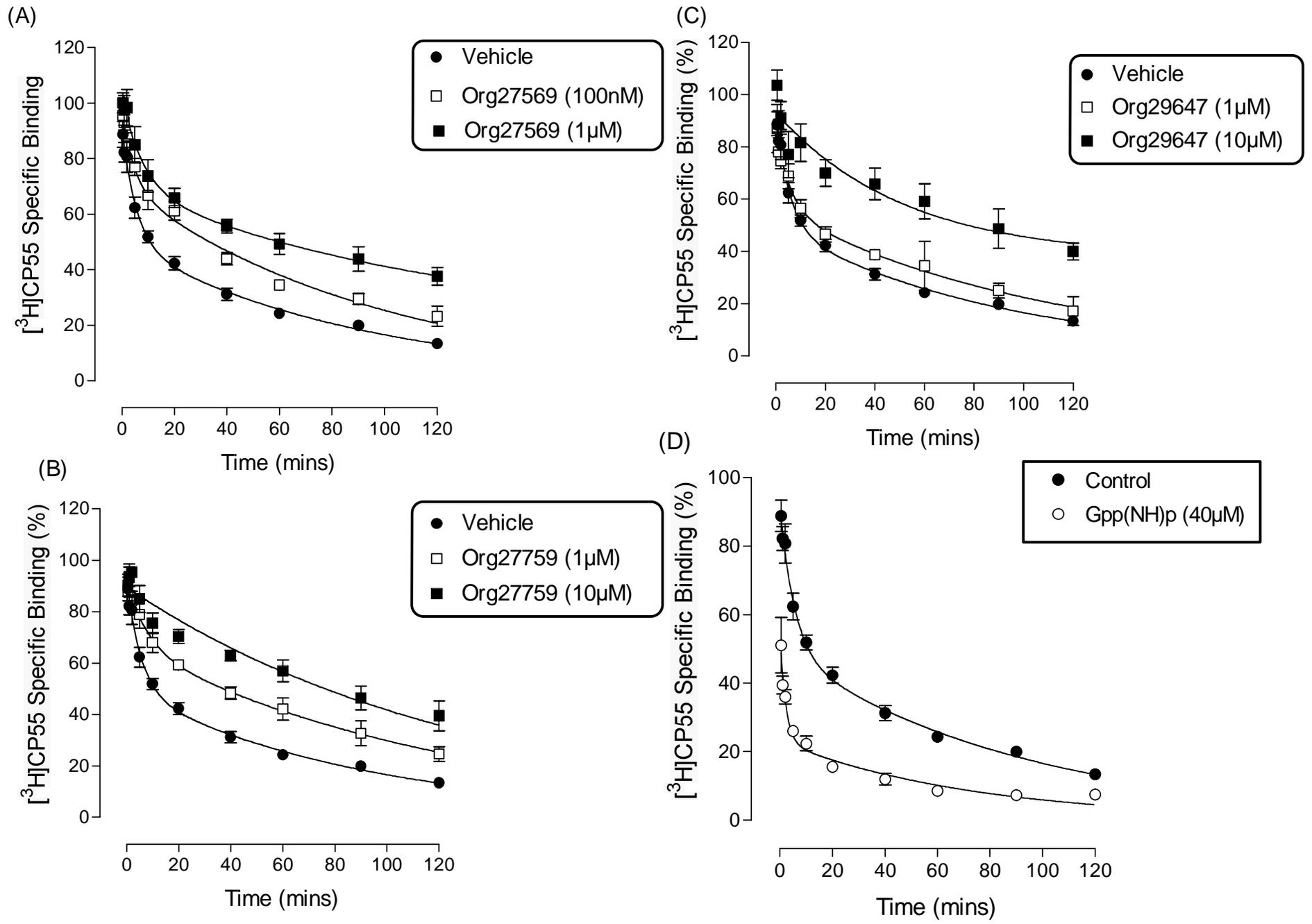
Figure 2

Org 27569

Org 29647
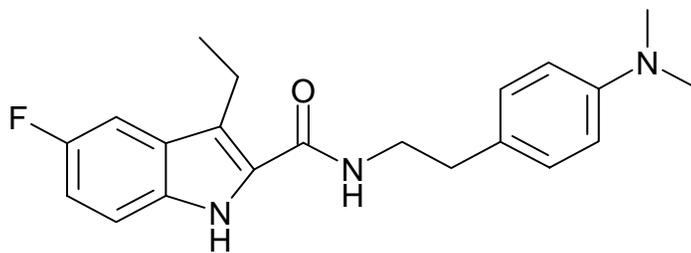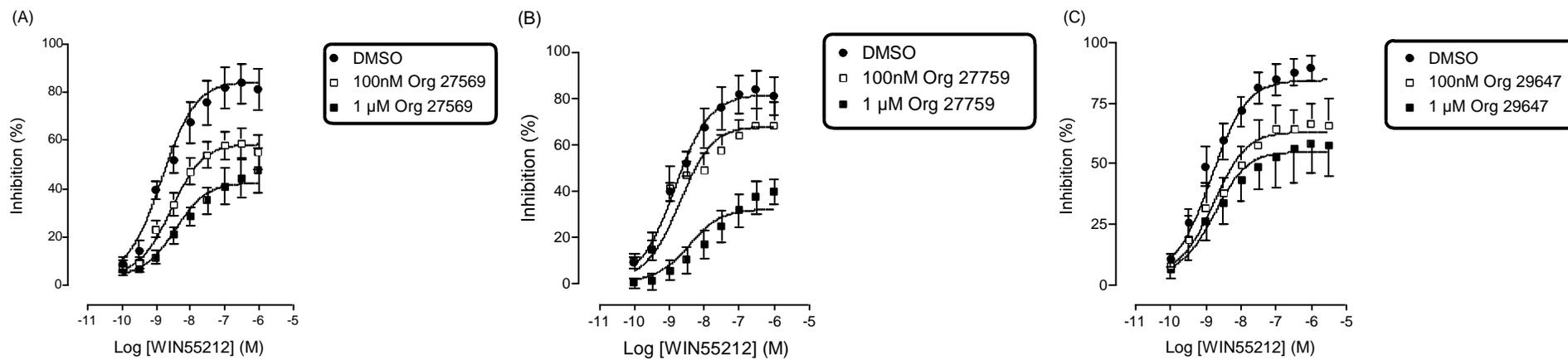
Org 27759

Figure 3

Figure 4

Figure 5

Figure 6

Figure 7

(A)

% change from basal (y-axis)
Log concentration CP55940 (M) (x-axis)

Legend:
● DMSO
□ ORG29647 (100nM)
○ ORG29647 (1μM)

(B)

% change from basal (y-axis)
Log concentration of anadamide (M) (x-axis)

Legend:
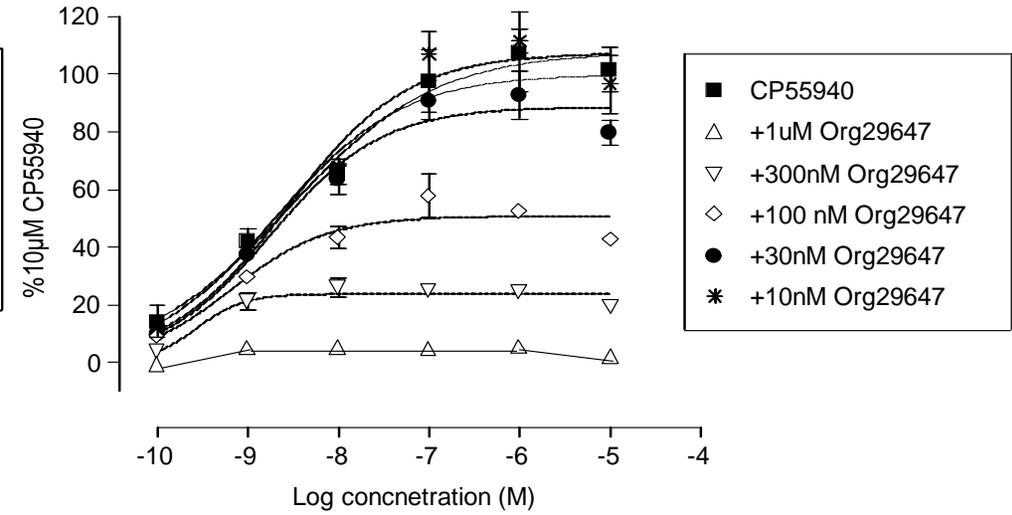● DMSO
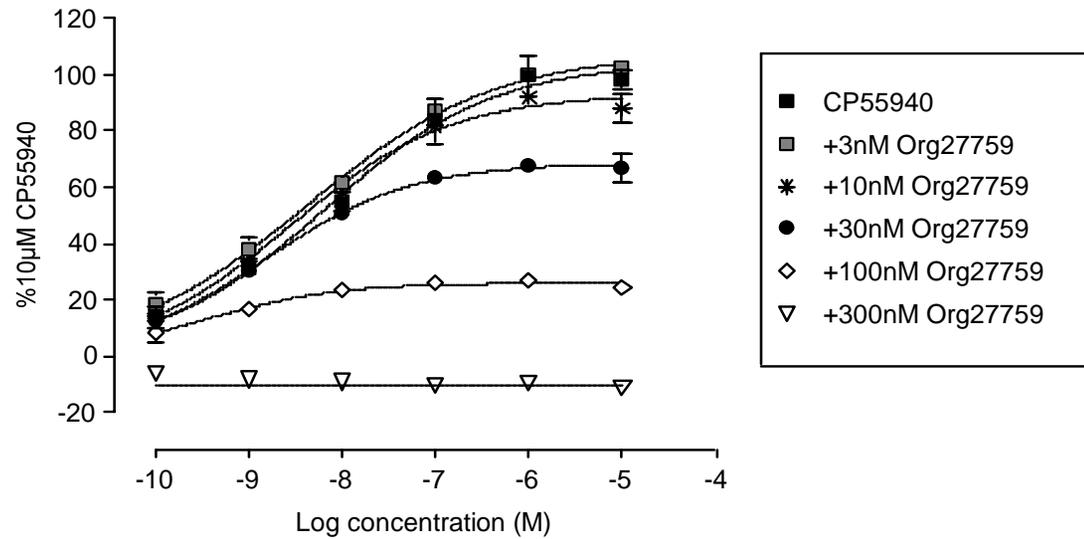□ ORG27569 (100nM)
○ ORG27569 (1μM)
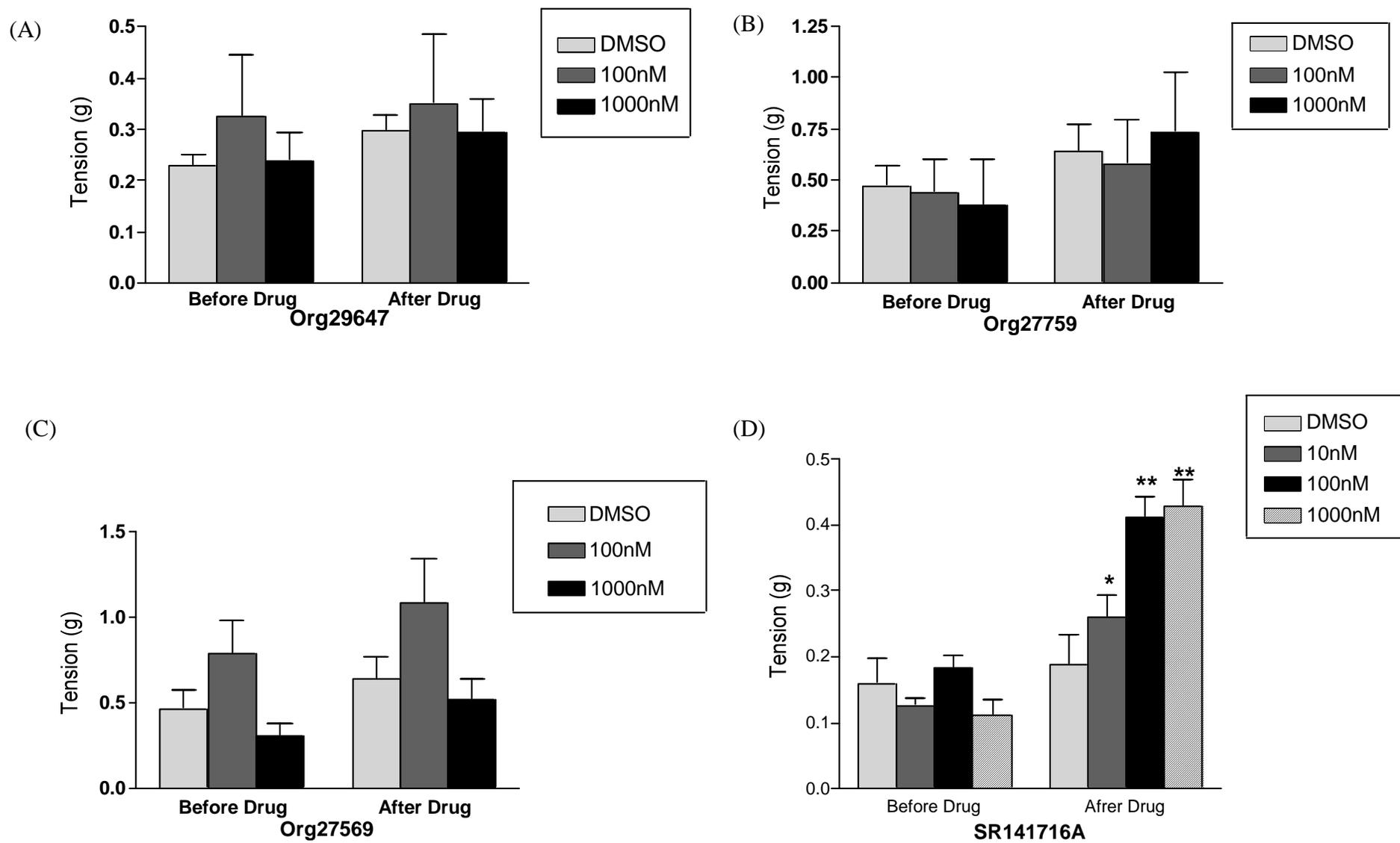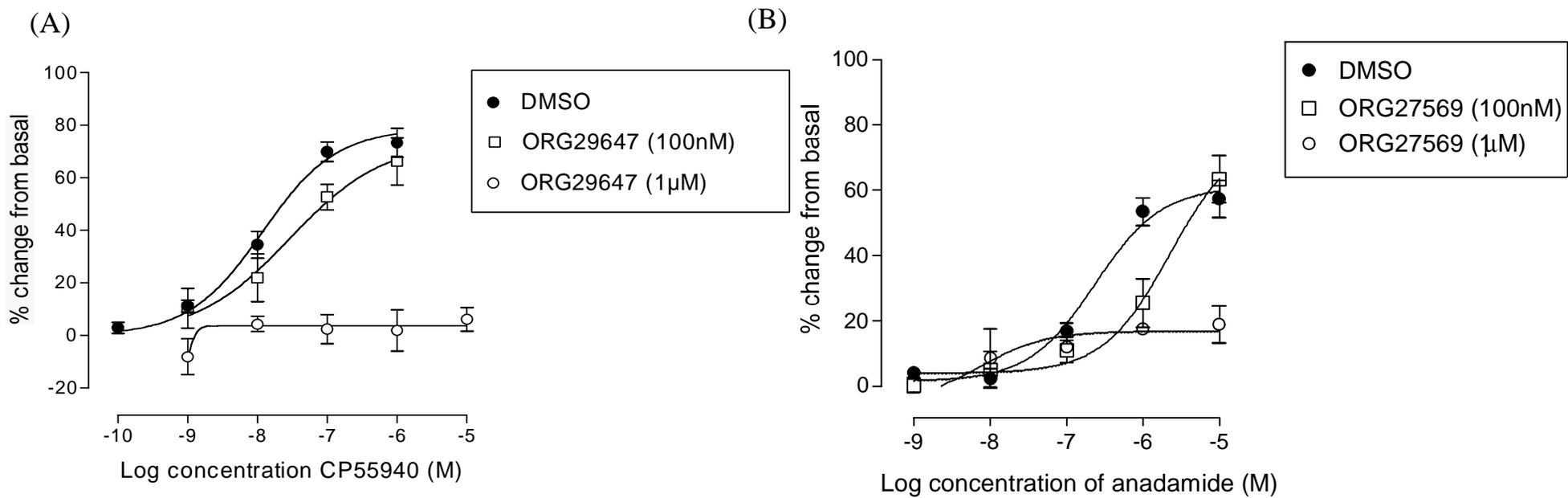
Figure 8

(A)
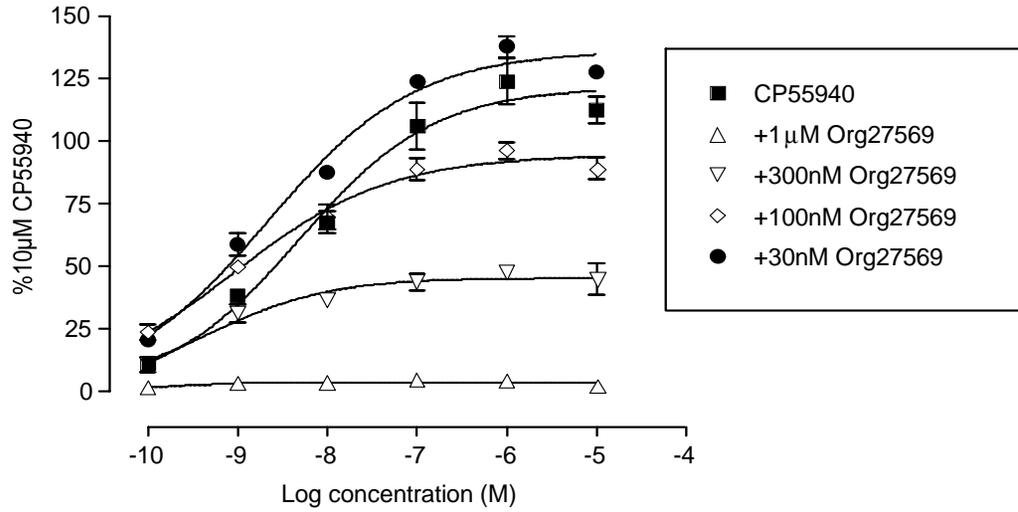
(B)

(C)

Appendix: An Operational Model of Allosteric Modulation

In the allosteric TCM (Figure 1), the orthosteric ligand, A, is distributed over two receptor-bound species, AR and ARB.   From this model, the concentration of the AR species in the presence of modulator, B, is as follows:

$$[AR] = \frac{[R]_T[A]}{[A]\left(1 + \frac{\alpha[B]}{K_B}\right) + K_A\left(1 + \frac{[B]}{K_B}\right)} \qquad (A1)$$

where $[R]_T$ denotes the total concentration of all receptor species (bound and unbound). Similarly, the concentration of the ARB ternary complex is described as:

$$[ARB] = \frac{[R]_T[A]}{[A]\left(1 + \frac{K_B}{\alpha[B]}\right) + K_A\left(\frac{1}{\alpha} + \frac{K_B}{\alpha[B]}\right)} \qquad (A2)$$

In addition to effects on ligand binding affinity, allosteric modulators may also affect the efficacy of orthosteric agonists.   In order to derive a functional model of allosterism that accounts for this possibility, it is first necessary to describe mathematically the effect of an allosteric modulator on the stimulus imparted by an orthosteric agonist to the cell, and the effect of stimulus-response coupling on the final observed response. In accordance with the conventions of classic receptor theory (Furchgott, 1966; Ehlert 1988), the stimulus (S) is equal to the product of the concentration of orthosteric agonist-occupied receptors and the agonist intrinsic efficacy.   In the presence of an allosteric modulator, the stimulus may thus be expressed as:

$$S = \ [AR] + \underline{\ } \ [ARB] \qquad\qquad (A3)$$

where   denotes the intrinsic efficacy of the orthosteric ligand and   is a coupling factor that describes the ability of an allosteric modulator to alter the signaling capacity of the [ARB] ternary complex. Values of   < 1 thus denote an attenuation in signaling, a situation that may be classed as a form of non-competitive antagonism of functional responses, values of   = 1 denote no change in the signaling capacity of the receptor in the presence of modulator and values of   > 1 denote an increased capacity of the receptor to signal in the presence of modulator. This model assumes that the allosteric modulator does not itself impart any stimulus to the receptor. Substitution of equations A1 and A2 into equation A3, followed by simplification, results in the following general form of the allosteric stimulus equation:

$$S = \frac{\varepsilon[R]_T[A]\left(1 + \dfrac{\alpha\beta[B]}{K_B}\right)}{[A]\left(1 + \dfrac{\alpha[B]}{K_B}\right) + K_A\ \ 1 + \dfrac{[B]}{K_B}} \qquad (A4)$$

To derive the relationship between agonist concentration and final tissue response, an allowance must be made for stimulus-response coupling. Since most relationships between occupancy and response are nonlinear in nature, equation A4 must be processed through a nonlinear function to derive an equation describing tissue response. One appropriate general function is the logistic equation, because it has been shown to closely model the shape of agonist concentration-response curves in many systems (Kenakin and Beek, 1982; Black and Leff, 1983). Thus, the tissue response (E), expressed as a fraction of the maximal response (E_m), may be described as a function of the stimulus as follows:

$$\frac{E}{E_m} = \frac{S^n}{K_S^{\ n} + S^n} \qquad (A5)$$

where the parameter, K_S, denotes a constant that governs the efficiency of stimulus-response coupling, and n denotes a logistic slope factor. Substituting equation A4 into equation A5, and defining $\_=$ $[R]_T/K_S$ as an operational measure of efficacy, gives the following operational model of agonism in the presence of an allosteric modulator:

$$E = \frac{E_m \tau^n [A]^n \left(1 + \dfrac{\alpha\beta[B]}{K_B}\right)^n}{[A]\left(1 + \dfrac{\alpha[B]}{K_B}\right) + K_A\left(1 + \dfrac{[B]}{K_B}\right)^n + \tau^n[A]^n\left(1 + \dfrac{\alpha\beta[B]}{K_B}\right)^n} \qquad (A6)$$